

TRANSPARENT GLAZES FOR PORCELAIN TILE: GLASSY AND GLASS-CERAMIC GLAZES WITH CRISTOBALITE CRYSTALLISATIONS

Sánchez-Muñoz, L.^(*), Cabrera M.J.^(**), Foo A.^(**), Beltrán H.^(*), Carda J.B.^(*)

^(*) Dept. of Inorganic and Organic Chemistry, Universitat Jaume I, Castellón

^(**) Vidres S.A., Villarreal, Castellón

ABSTRACT

As result of the collaboration between the company Vidres S.A. and the Dept. of Inorganic and Organic Chemistry of Universitat Jaume I of Castellón, frits have been developed of a glassy and glass-ceramic nature (with crystallisation of chemically stabilised -cristobalite), which can be used in transparent glaze compositions for porcelain tile, with the possibility of polishing. Both the glassy and the glass-ceramic glazes have been developed in the system $\text{SiO}_2\text{-Al}_2\text{O}_3\text{-B}_2\text{O}_3\text{-CaO-ZnO-Na}_2\text{O-K}_2\text{O-BaO-SrO}$ with contents in SiO_2 up to 73 wt%, using raw materials typically found in the ceramic industry. Crystallisation of cristobalite of composition $\text{Si}_{1-x}\text{Al}_x\text{Sr}_{x/2}\text{O}_2$ and $\text{Si}_{1-x}\text{Al}_x\text{Ca}_{x/2}\text{O}_2$ takes place by heterogeneous nucleation at the glaze surface and at the frit particle contact points, growing first as regular isolated crystals and then as dendritic crystals, in which case they can occupy large surface areas of the glaze. The glazes developed, in which these frits are the fundamental component, have higher mechanical properties with regard to hardness, resistance to abrasion, acids and stains than conventional transparent glazes and the porcelain tile polished surface.

1. INTRODUCTION

Industrial materials of the porcelain tile type (tiles with ceramic bodies whose water absorption is less than 0.5 % by weight) have progressively evolved with time. At first, production basically consisted of unglazed bodies, either with a natural or polished surface, where the decoration was performed in mass or using soluble salts at the surface. One of the main problems of the polished bodies is that this process exposes previously closed porosity inside the body, so that irreversible stains can appear associated with the dirt held in these pores. However, at present a very important part of production is marketed with a glazed surface, enabling traditional decorating techniques to be used and optionally also polishing.

In most cases, the glazes used are transparent ones of the glassy type and opaque ones of the crystalline type (i.e., white glazes made with additions of zircon opacifiers). With a view to improving surface mechanical properties, in the last few years white glazes have been developed for porcelain tiles of the glass-ceramic type^[1,2,3], i.e., glassy glazes that partly crystallise during the firing cycle of the tile they coat^[4,5,6]. It is clear that opaque glazes hide the body, and hence the existence of polishable transparent glazes with good mechanical properties (i.e., glass-ceramic glazes) would be interesting for tiles with in-mass decoration (eliminating the problem of the closed porosity in the body appearing at the surface) and with traditional screen printing decoration. On the other hand, it is known that with the same chemical and mineralogical composition, adding minerals to a coating (i.e., in the crystalline glazes) does not provide the mechanical properties found when the crystals form in the glaze (i.e., in the glass-ceramic glazes).

Excluding the effect of heterogeneities such as porosity or the effect of liquid immiscibility, the transparency or opacity of the glass-ceramic glazes, depends mainly on two factors: i) abundance and crystal size distribution of the crystalline material and, ii) difference of refractive index between the crystals and the glass. When crystal size is smaller than incident radiation wavelength (i.e., visible light), transparent materials are found^[7,8]. However, this method requires accurate control of crystallisation conditions, which involves adapting tile firing cycles to the needs of the glaze, this being difficult to imagine in the tile industry, where firing cycles are designed for appropriate sintering of the body and profitability of the process. Therefore, to develop glass-ceramic glazes adapted to the porcelain tile firing cycles it is convenient to investigate crystallisation processes of crystalline phases whose refractive index is very close to that of the glass.

Based on the economic availability of the raw materials and taking into account that the refractive index n of the glasses based on SiO_2 and B_2O_3 lies between 1.4 and 1.5, there are very few crystalline phases that can crystallise in a glass-ceramic glaze with a refractive index similar to that of the glass. In this sense, previous studies and the experience of a working group have shown that crystallisation in glass-ceramic systems for glazes of corundum^[3] Al_2O_3 ($n = 1.77$), spinel^[1,2] MgAl_2O_4 ($n = 1.72$), diopside^[9] $\text{CaMgSi}_2\text{O}_6$ ($n = 1.67$), mullite^[3] $\text{Al}_6\text{Si}_3\text{O}_{18}$ ($n = 1.64$), wollastonite CaSiO_3 ($n = 1.63$), celsian^[1,2] $\text{BaAl}_2\text{Si}_2\text{O}_8$ ($n = 1.59$), and even anorthite^[1,2] $\text{CaAl}_2\text{Si}_2\text{O}_8$ ($n = 1.58$), give rise to opaque and translucent glazes depending on the degree of crystallisation. Obviously, the additions of nucleating agents also help achieve opacity. Therefore, in this study it was decided to address the development of glass-ceramic glazes in which the major phase in crystallisation was cristobalite, whose refractive index is about 1.5,

without the addition of nucleating agents. With this objective, frits have been developed with a high silica content for use in cristobalite glass-ceramic glazes, i.e., which enable the formation of these crystals during porcelain tile single-firing cycles.

This type of frits has a series of further advantages, of which the following are particularly noteworthy: i) a high silica content means a low materials cost in the final product; ii) the formulations enable the use of simple, common raw materials in the ceramic industry; iii) owing to the ease with which cristobalite forms, suitably proportioning the remaining frit components allows producing a wide range of glazes with different crystallisation capacities; iv) given the low reactivity of silica, glazes can be designed with additions of other minerals to the starting frit, without undesirable mineral phases forming.

On the other hand, high silica contents involve certain disadvantages relating to this type of glazes, particularly: i) the melting temperature must be as high as possible; ii) there is a notable difficulty in producing a frit (glass) with a homogeneous chemical composition, iii) owing to the sought transparency nucleating agents (TiO_2 , ZrO_2 , P_2O_5 , CeO_2 , etc.) cannot be used, as they are compounds with a very high refractive index and give rise to opacity; iv) important, abrupt changes can occur in volume (shrinkage) owing to the $\beta \rightarrow \alpha$ transformation during cooling. This last drawback needs to be dealt with in detail to explain how this has been solved.

Cristobalite is a SiO_2 polymorph whose structure can be described by stacks of layers (formed by linked rings of six units of silicon tetrahedrons with alternating apical oxygens, Fig. 1a) in an arrangement ABC-ABC... (Fig. 1e) and in a "trans" orientation (Fig. 1c). The structure of tridymite is similar to this, but with layer stacking according to an order AB-AB... (Fig. 1d) and "cis" orientation (Fig. 1b). Cristobalite has a very open structure with large holes in the centre of the interface hexagon between two ABC sheets. As a result, this has a phase transition of the structural collapse type between a high temperature $Fd3m$ cubic symmetry (β -phase) and a low temperature $P422$ tetragonal symmetry (α -phase), of the displacement type and reversible at about 273 °C, with a change in the structure angle distribution T-O-T and formation of a domain structure^[10-15]. During the transition, owing to the collapse indicated of the three-dimensional tetrahedron frame, an important volume decrease (2.8 %) occurs in cooling (and hence of expansion in heating) with important well-known consequences from a ceramic point of view. The partial substitutions of Si by Al in the tetrahedral holes allow incorporating cations in the large structural holes mentioned before, for local charge compensation (Fig. 1f). These cations situated between the interstices act as anchors that can partly inhibit the collapse of the structure and therefore delay transition advance. When this type of structure is produced by partial substitution of Si by Al plus one +1 and/or +2 cation, its X-ray diffraction (XRD) diagrams at room temperature are similar to those of β -cristobalite, called chemically stabilised β -cristobalite (CSC), i.e. advance has been impeded of the $\beta \rightarrow \alpha$ phase transition^[16-20]. The use of glass-ceramic materials with CSC-type cristobalite, employing its high resistance to thermal shock, is well known^[21,22]; however owing to the chemical composition used, higher temperatures than 1750 °C were required to homogenise the chemical composition of the starting glass, besides the arising mullite crystallisation^[21]. This could be why, according to information available to the authors, these materials have not been used to date as glazes for tiles or other types of traditional ceramics, to produce transparency and contribute physical and chemical resistance properties.

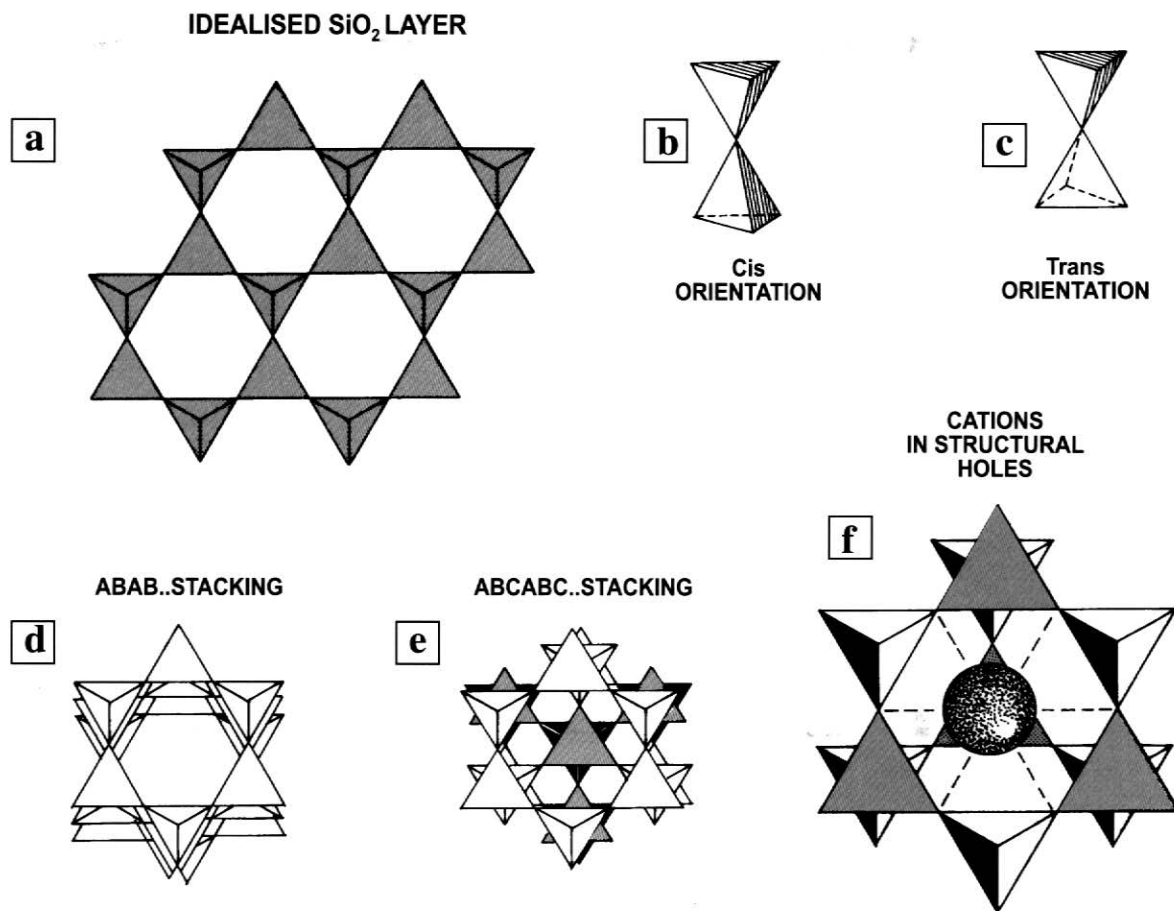


Fig. 1.- a) Scheme of the layers of silicon tetrahedrons forming hexagonal rings, whose apical oxygens are found in an alternate arrangement; b) "cis" orientation in which two layers of tetrahedrons are linked by apical oxygens connected by an "m" symmetry plane; c) ditto "trans" but in this case they are connected by a "2" axis; d) scheme of tridymite type structures formed by layer stacking according to an order ABAB... in "cis"; position e) scheme of the cristobalite-type structures formed by layer stacking according to an order ABCABC... in "trans" position; f) scheme of the position that stabilising cations occupy in the cristobalite-type structure in the interface between two ABC sheets in the centre of a hexagonal ring.

The appearance of the α -phase in glasses and ceramics has always been considered a problem and their chemical compositions are usually adapted to avoid such formation^[23,24]. The study sets out how these disadvantages have been solved in the synthesis of frits and in CSC crystallisation to develop transparent glass-ceramic glazes.

2. WORK METHODOLOGY

The following work programme was established to achieve objective set:

i) First, the experimental results found in the literature on the chemical stabilisation of cristobalite β at room temperature were reproduced, then extending the compositional ranges, and later the ideal thermal treatments. For this, the sol-gel method was used, with the coprecipitation technique. This information was then used for the development of the frits.

ii) Secondly, frits were prepared with a high silica content at the usual melting temperatures found in the ceramic sector, i.e. around 1500 °C, using the appropriate raw materials and fluxes.

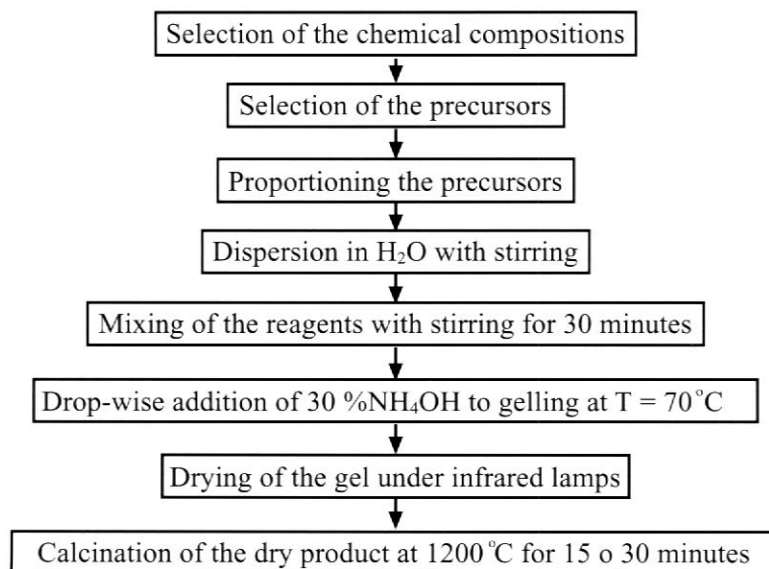
iii) Thirdly, the capacity of cristobalite to crystallise from the frits was confirmed, as well as the crystallisation extent and formation processes when using porcelain tile firing cycles.

iv) Fourthly, glaze behaviour was optimised in relation to its meltability, stretching and maturing by additions to the frit of industrial minerals such as quartz, alkaline feldspars, kaolin and alumina.

2.1. CSC SYNTHESIS BY COPRECIPITATION

The sol-gel method has already been used for the synthesis of cristobalite^[16-20]. Specifically, the CSC formation capacity has been observed by substituting Si by Na+Al^[16,19], Ca+Al^[16-22], Cu+Al^[19] and Al+Sr^[19]. In this study, stabilisation by Na+Al was discarded owing to the difficulty of obtaining quality glazes at porcelain tile firing temperatures, and by Cu+Al owing to the type of raw materials required.

Using soluble salts of the precursor materials, a solution was prepared to which an agent was added that gives rise to the formation of insoluble salts or hydroxides of the ions involved, or their simultaneous precipitation. This enables achieving an important degree of mixing of the components and compositional homogeneity, and even if the first case occurs, also achieving part of the pairs of bonds between the ions that are sought in the structure. The phases involved in producing cristobalite by this technique are set out in the following flow diagram:



The chemical compositions chosen to form the CSC structure consist of the partial substitution of Si by Al+Sr or by Al+Ca, according to the respective formulas $\text{Si}_{1-x}\text{Al}_x\text{Sr}_{x/2}\text{O}_2$ and $\text{Si}_{1-x}\text{Al}_x\text{Ca}_{x/2}\text{O}_2$.

The chemical precursors of these compositions were colloidal silica for SiO_2 , aluminium nitrate $\text{Al}(\text{NO}_3)_3 \cdot 9\text{H}_2\text{O}$ for Al_2O_3 , strontium carbonate SrCO_3 for SrO, and calcium nitrate $\text{Ca}(\text{NO}_3)_2 \cdot 4\text{H}_2\text{O}$ for CaO.

The proportioning was designed to produce chemical compositions in which $x = 0.03, 0.05, 0.06, 0.08$ and 0.09 for stabilisation with Sr and $x = 0.03, 0.05, 0.06, 0.08, 0.09, 0.11, 0.13$ and 0.15 for Ca.

The precursors of Al and Sr, and the colloidal silica were each separately dispersed in 50 mL of distilled water for 15 minutes. They were then mixed by stirring for 30 minutes for good quality dispersion. 30 % ammonium was subsequently added drop-wise to this colloidal dispersion, holding mixture temperature at 70 °C, until achieving destabilisation with gel formation. This was slowly dried under infrared lamps and then calcined at 1200 °C with holding times of 15 and 30 minutes.

2.2 PREPARATION OF THE FRITS AND THEIR APPLICATION

The frits were developed in the system $\text{SiO}_2\text{-B}_2\text{O}_3\text{-Al}_2\text{O}_3\text{-CaO-SrO-K}_2\text{O-Na}_2\text{O-MgO-ZnO-BaO}$. As the purpose of the frits is their crystallisation as cristobalite, frits with a high SiO_2 content were used, in certain cases up to 73 % by weight. Also fundamental are Al_2O_3 , CaO and SrO as cristobalite-forming elements. The oxides B_2O_3 , Na_2O , K_2O , ZnO, BaO and MgO were chosen as fluxes to obtain the fritted products at temperatures around 1500 °C. The fundamental difference between the frits rich in Na_2O compared to those with a high K_2O content is that in the former, more cristobalite crystallises. The alumina concentration also plays a regulating role in crystallisation, as it inhibits cristobalite formation at high concentrations. When CaO and ZnO contents are excessive, CaSiO_3 calcium silicates form of the wollastonite type, and Zn_2SiO_4 zinc silicates of the willemite type, that produce opacity.

Owing to the high silica content of the chemical formulas involved, problems of homogeneity occurred, which were solved by selecting appropriate raw materials. In this sense quartz was added in the smallest possible quantities, mainly using silicates of the alkaline and alkaline-earth elements, instead of carbonates or nitrates.

After mixing and homogenising the raw materials in a ball mill, they were fritted in an alumina crucible in laboratory fritting kilns, producing enough material to make the glazes and perform the tests on application onto green commercial porcelain tile bodies and other made by the company Vidres S.A. The glazed pieces were fired in industrial single-fire kilns, placing them in the production lines to ensure having results that were industrially reproducible.

2.3. INSTRUMENTAL TECHNIQUES

Both the frits and gels were studied by differential thermal analysis (DTA) (Mettler-Toledo 851) at heating rates of 25 °C/min to have data on crystallisation start and its repetition in the various formulations.

The gels subjected to heat treatment and the fired pieces were studied by X-ray diffraction (XRD) (Siemens D5000) to identify the crystalline phases that formed, working at 40 KV and 20 mA, with different scanning velocities and time constants as a function of each test. It should be noted that the XRD diagrams of synthesised cristobalites in the

systems $\text{SiO}_2\text{-Al}_2\text{O}_3\text{-SrO}$ and $\text{SiO}_2\text{-Al}_2\text{O}_3\text{-CaO}$ were compared with the ASTM files corresponding to cristobalite of composition SiO_2 , i.e., file no. 39-1425 for the α -phase and file no. 27-0605 for the β -phase.

The microtextures relative to the porosity of the glaze and the crystallisations were studied by scanning electron microscopy (SEM) (LEO 6300). To obtain the images, secondary electrons were used and especially backscattering electrons which, owing to the difference in chemical composition between glass and crystals, enabled obtaining clear images with regard to the distribution of both phases. This study was done with the help of energy-dispersive microanalysis EDAX (Oxford, Link model), which enables comparing the chemical composition of the crystals and the glass in the glass-ceramic glazes.

2.4. MEASUREMENT OF GLAZE PROPERTIES

The properties studied in the glazes were hardness (with a Vickers microhardness tester and with the Mohs hardness test according to standard UNE 67 101), abrasion resistance (standard UNE EN ISO 10545-7), chemical resistance (standard UNE 67 122), and stain resistance (standard UNE 67 11/85).

3. RESULTS AND DISCUSSION

3.1. CRYSTALLISATION OF CRISTOBALITE FROM THE GEL

As mentioned in the introduction, in this study it was decided to produce CSC in two compositional systems: $\text{SiO}_2\text{-Al}_2\text{O}_3\text{-SrO}$ according to the formula $\text{Si}_{1-x}\text{Al}_x\text{Sr}_{x/2}\text{O}_2$ and $\text{SiO}_2\text{-Al}_2\text{O}_3\text{-SrO}$ according to the formula $\text{Si}_{1-x}\text{Al}_x\text{Ca}_{x/2}\text{O}_2$. The values of x at which crystallisation of cristobalite occurred in the first case were $x = 0.03, 0.05, 0.06, 0.08$ and 0.09 , while in the second these were $0.03, 0.05, 0.06, 0.08, 0.09, 0.11, 0.13$ and 0.15 . In both cases and in all the compositions, the heat treatment applied (1200°C for periods of 15 and 30 minutes) yielded cristobalite crystallisation, though in the system with Ca crystallisations occurred more rapidly and crystals of greater crystallinity formed, as can be inferred from the characteristics of the XRD diagrams.

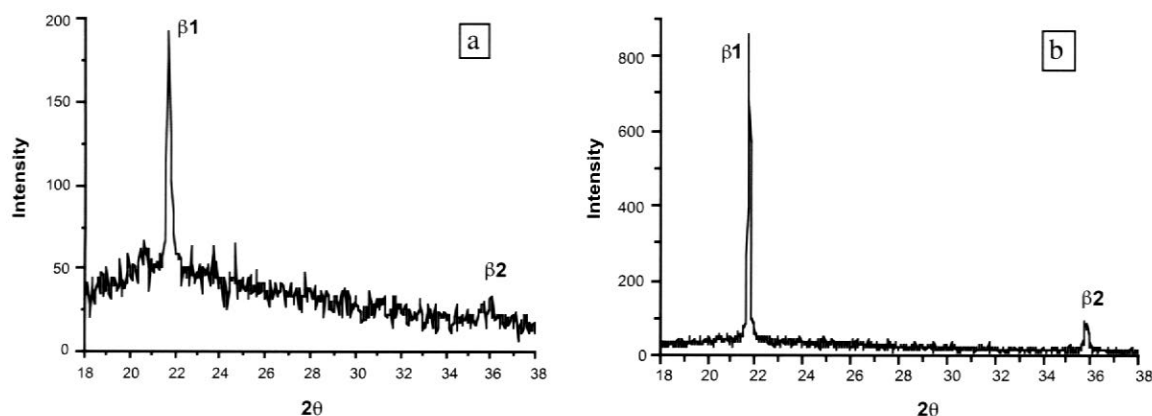


Fig. 2.- XRD diagrams gels calcined at 1200°C for 15 minutes in the composition $\text{Si}_{0.97}\text{Al}_{0.03}\text{Sr}_{0.015}\text{O}_2$ (a) and $\text{Si}_{0.95}\text{Al}_{0.05}\text{Ca}_{0.025}\text{O}_2$ (b). The values of the 2θ angle and \AA spacing are given Table I, except for peak β_2 of figure b, as it is not well defined.

Fig. 2a shows an XRD diagram for composition $\text{Si}_{0.97}\text{Al}_{0.03}\text{Sr}_{0.015}\text{O}_2$ with crystallisation of a structure similar to β -cristobalite i.e., CSC. Fig. 2b shows an XRD diagram for composition $\text{Si}_{0.95}\text{Al}_{0.05}\text{Ca}_{0.05}\text{O}_2$ in which the same type of structure forms. The details of the gel crystallisation processes at different temperatures will be set out in another paper. In this study, the foregoing results have allowed us to infer the possibility of CSC formation from variable chemical compositions at porcelain tile firing temperatures in relatively short times, and it is therefore useful to attempt to reproduce this crystallisation from ceramic frits.

At this point it should be noted that the arising CSCs have XRD diagrams with the same peaks as the β -phase, but slightly shifted because stabilisation has been partial. This is because during phase transition the structure collapses more with a smaller stabilising cation content, and therefore the position of the β_1 and β_2 maximum values vary slightly depending on the chemical composition. In this sense, full stabilisation, i.e., when no differences are observed between the diagram of a SiO_2 cristobalite in the standard -phase and synthetic cristobalite in the system $\text{SiO}_2\text{-Al}_2\text{O}_3\text{-CaO}$, corresponds to values of $x = 0.15$ ($\text{Si}_{0.85}\text{Al}_{0.15}\text{Ca}_{0.075}\text{O}_2$). As the values of x decrease, the difference between the positions of these two phases rises, i.e., a lower degree of chemical stabilisation is attained.

3.2. GLASSY AND GLASS-CERAMIC GLAZES

Two examples follow of glazes exclusively made up of frits, produced in industrial porcelain tile firing cycles at 1200 °C, illustrating the materials that have been developed.

Fig. 3a shows an image made by SEM of a glaze comprising a frit in which crystallisation has not taken place, thus presenting a homogeneous appearance. It is to be noted that there is no engobe, while the glaze layer is quite thick, and the relative quality in the degree of sintering is evidenced by few flaws. Owing to the great transparency achieved, this type of glaze can be used in polishing processes, which enhance glaze gloss compared with natural surfaces.

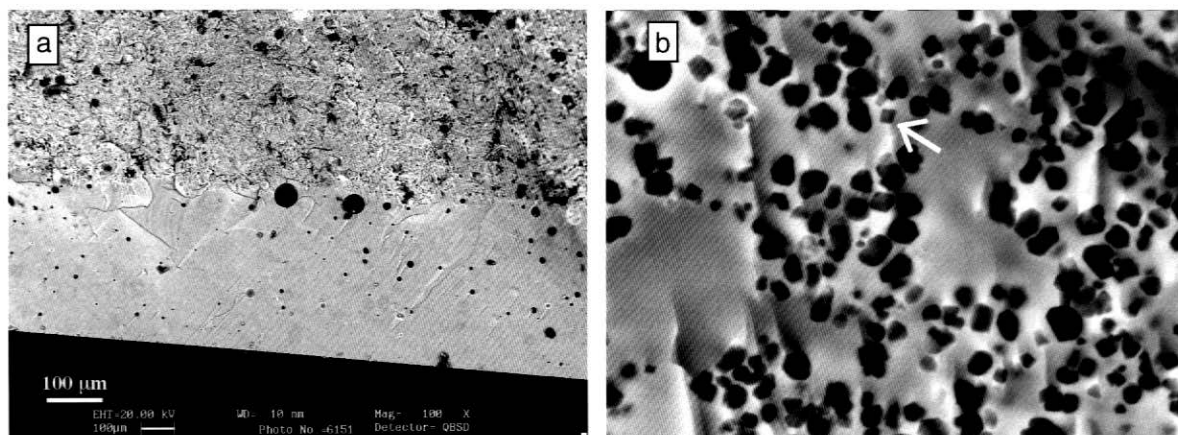


Fig. 3.- The SEM micrographs, made using the backscattered electron detector, of a glaze comprising a frit that does not crystallise (a) showing the homogeneity and relative sintering quality of the glaze without engobe. Figure (b) shows microtexture detail of a glass-ceramic glaze in which isolated crystals appear, some of which have an octahedral morphology (marked with an arrow).

Fig. 3b depicts a SEM micrograph of the glass-ceramic glaze (in which the backscattered electron technique enables registering compositional differences between the glass and the crystals), where dark-coloured regular crystals are observed, all with similar sizes between 1 and 3 μm , immersed in a light-coloured glassy matrix. The characteristics of the arising crystallisation are set out in following sections.

It may be mentioned here that regulating the starting frit compositions has enabled establishing a wide compositional range in the system $\text{SiO}_2\text{-B}_2\text{O}_3\text{-Al}_2\text{O}_3\text{-CaO-SrO-K}_2\text{O-Na}_2\text{O-MgO-ZnO-BaO}$, in which crystallisation of cristobalite occurs, and CSC is found at room temperature. In particular, the frits rich in CaO crystallise better than those rich in SrO, the presence of B_2O_3 and Na_2O favouring crystallisation while K_2O , MgO and ZnO inhibit this. This is due to the decrease in glaze viscosity at peak firing temperature by part of the Na and B atoms, which increases cation diffusion and thus crystallisation. An excess of these elements has the opposite effect, as the frit melts excessively, producing glaze stretching problems. Alumina plays a key role, as it considerably modifies viscosity, with high values inhibiting crystallisation, while low values keep this cation from entering the cristobalite network so that no CSC can arise.

3.3. CRISTOBALITE CRYSTALLISATION FROM A FRIT

The ability of the frits to crystallise is clearly demonstrated in the DTA diagrams. When one of the developed frits has the capacity to crystallise (Fig. 4), the DTA diagram, besides indicating the glass transition temperature T_g and melting temperature T_f , presents a broad, poorly defined exothermic peak that begins a little after T_g and maximises around 900 $^\circ\text{C}$. The position of this maximum varies in the studied frits between 875 and 990 $^\circ\text{C}$, but always has a similar shape to the one shown in Fig. 4. This shape differs from that of materials in which some nucleating agent has been used in the formulation, in which case finer, better defined exothermic peaks are found that however give rise to opacity in the glaze.

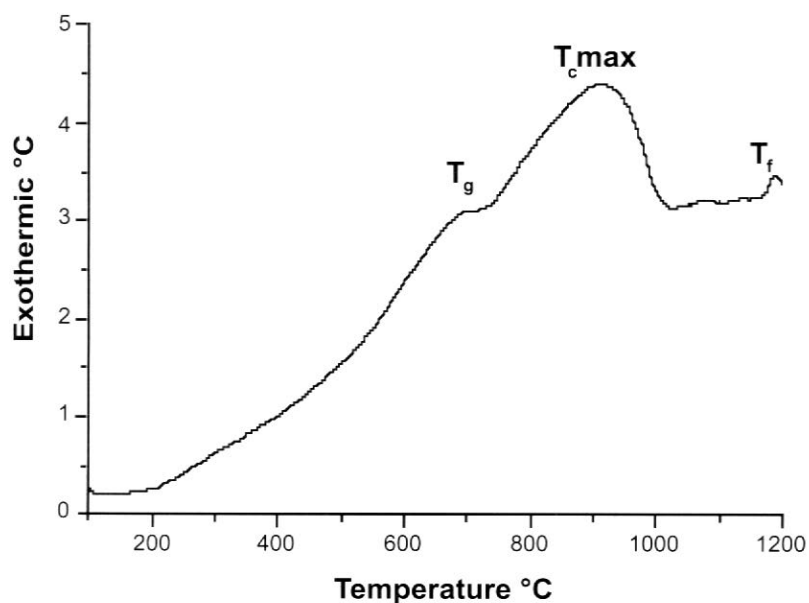


Fig. 4.- DTA diagram of a frit with glass-ceramic behaviour. The glass transition and melting temperature are respectively marked as T_g and T_f . $T_c \text{ max}$ is the maximum exothermic temperature caused by the crystallisation process. Heating rate 25 $^\circ\text{C}/\text{minute}$.

3.4. GLASS-CERAMIC GLAZES

Fig. 5a shows the XRD diagram of a glaze completely made up of a frit rich in SrO, i.e., in which β -cristobalite has crystallised in the system $\text{SiO}_2\text{-Al}_2\text{O}_3\text{-SrO}$. To be noted is the poor definition and low intensity of the diffraction peaks compared to those of a frit rich in CaO of the system $\text{SiO}_2\text{-Al}_2\text{O}_3\text{-CaO}$ (Fig. 5b), corresponding to a glaze completely made up of this frit with additions of quartz (marked with Q in this figure). In these cases, the position of the diffraction peaks $\beta 1$ and $\beta 2$ is closer to the values measured at high temperature of the β -cristobalite of standard SiO_2 type (Table I) than to those of the position of type α (Table II).

	$\beta 1$	$\beta 2$
β -cristobalite SiO_2^*	21.620, 4.110	35.640, 2.517
β -cristobalite Fig. 2a	21.695, 4.093	-
β -cristobalite Fig. 2b	21.727, 4.087	35.789, 2.506
β -cristobalite Fig. 5a	21.612, 4.108	35.633, 2.517
β -cristobalite Fig. 5b	21.690, 4.090	35, 770, 2.508

(*ASTM File no. 27-0605)

Table 1. Values of the 2θ angles and d spacings in \AA measured in the mean position of the peak at half height in the XRD diagrams of the samples indicated in the text ($\text{Cu K}\alpha_1$ radiation).

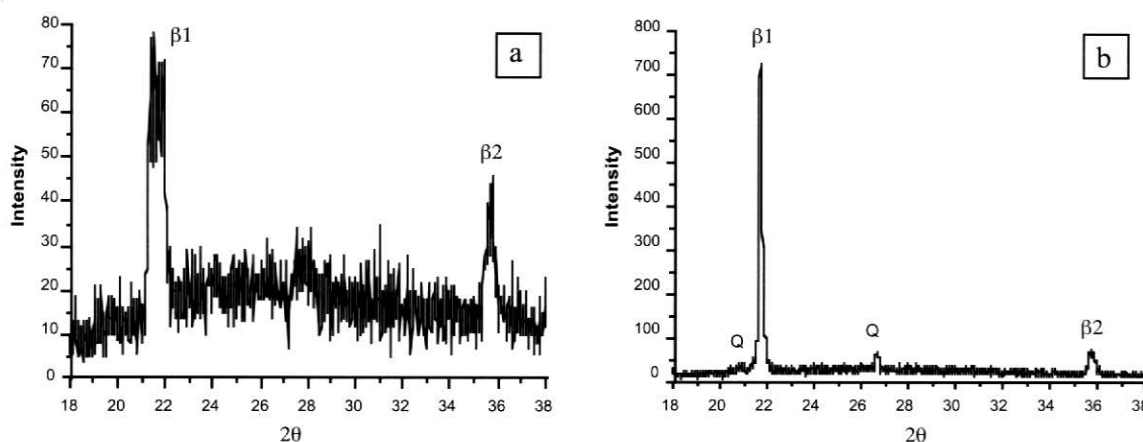


Fig. 5.- XRD diagrams of two frits with glass-ceramic behaviour, a) frit based on the system $\text{SiO}_2\text{-Al}_2\text{O}_3\text{-SrO}$ showing the formation of a CSC with a highly heterogeneous character, which explains the width of the lines; b) glaze made up of a frit based on the system $\text{SiO}_2\text{-Al}_2\text{O}_3\text{-CaO}$ and quartz (peaks marked by Q).

Glaze crystallisation has not been homogeneous throughout the applied layer thickness owing to different nucleation mechanisms that condition crystal formation. Fig. 6a shows the microtexture inside the glaze, i.e., between the surface and the body. In this inner part, an irregular distribution can be observed, along guiding lines that give rise to separate regions without crystallisation. This distribution is caused by crystallisation occurring at grain boundaries of frit particles before sintering, as in these zones flaws accumulate that serve for a heterogeneous nucleation process.

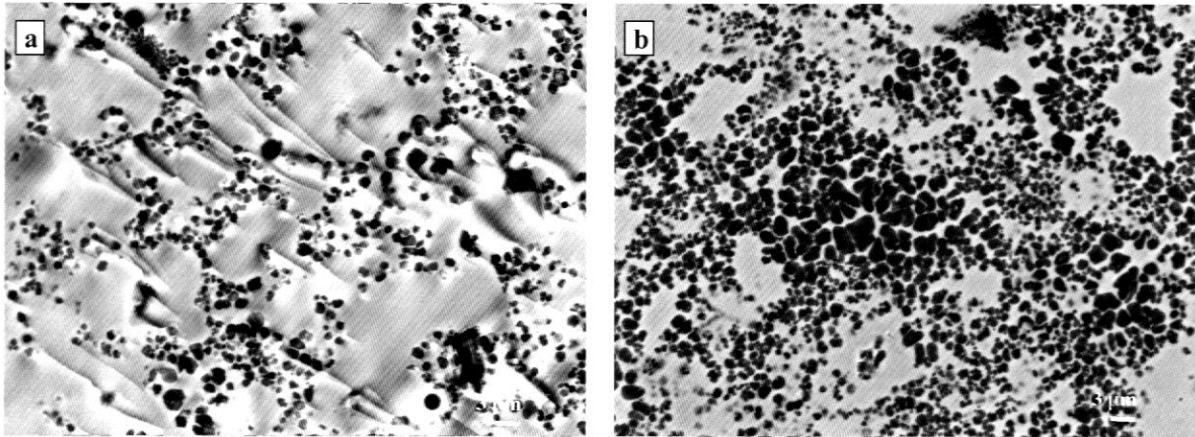


Fig. 6.- SEM micrographs using the backscattered electron detector with the same magnification (2000x). a) Microtextures observed inside the glaze layer, where crystals accumulate in linear regions that correspond to previous intergranular contacts of the frit. b) Microtextures observed at the glaze layer surface, where the crystals present an irregular distribution.

However, when the glaze surface is observed (Fig. 6b) larger areas of crystallisation appear, with larger-size crystals than inside, as well as regions without crystallising that resemble those of the inner regions. It is therefore clear that surface nucleation is primarily involved, encouraged by the surface flaws of the frit particles or by those created at these interfaces at sintering start. Isolated crystals are observed to appear in the centre parts of the individual regions mentioned before, both inside the glaze and at the surface, which are interpreted as homogeneous nucleation processes, though these processes are much less widespread than the other two.

When images are made of microtextural details with backscattered electrons, clearer contrasts can be observed in the parts surrounding the crystals than in the centre parts of these darker homogeneous regions (Fig. 7). This effect is interpreted as involving chemical composition gradients around the crystals generated by diffusion processes for crystalline growth, i.e., the crystals grow by atomic diffusion and not by interface processes, as was to be expected given the difference in chemical composition between melt and crystal.

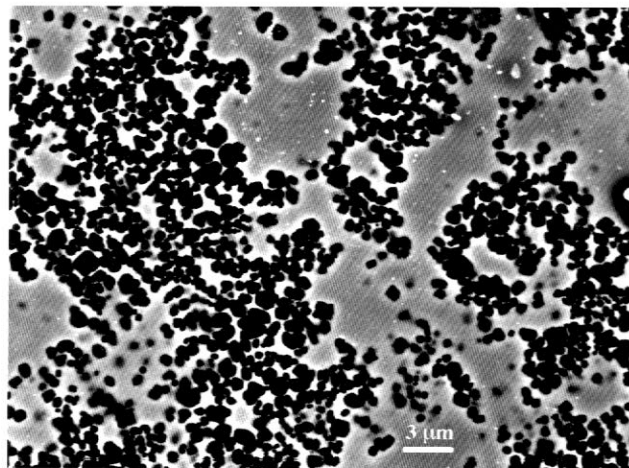


Fig.7.- SEM micrographs using the backscattered electron detector at a magnification of 2500x, showing three colours: black for the crystals, grey for the glass and a light colour for the contact zones between the crystals and the glassy matrix.

On performing spot chemical analysis by EDAX on the crystals and glassy matrix, the role of each element in the formation of the glass-ceramic material can be appreciated. In this sense the frit composition can be divided into three groups of components:

i) Fundamental SiO_2 component, in which crystal concentration always exceeds that of the glassy matrix, with over 75 % by weight in crystals and less than this value in the glass.

ii) β -cristobalite stabilising components that need Al instead of Si for the entry of cations +1 and 2+ in the irregular holes of the three-dimensional tetrahedron frame of the cristobalite structure. The Al_2O_3 concentration in the crystals is smaller than 5 % by weight and higher than this value in the glass. It has also been observed that not just Ca and Sr enter the crystal structure, but Na, Zn and Ba can also participate in the cristobalite chemical stabilisation processes, though in much smaller concentrations than Ca and Sr. All these elements are always found in larger concentration in the glass than in the crystals.

iii) Residual components that do not participate in the crystals but help adapt the characteristics of the glaze to the body, as well as for the melting of the raw materials, such as B_2O_3 (which cannot be measured by EDAX) and MgO.

3.5. $\beta \rightarrow \alpha$ TRANSFORMATIONS IN THE GLAZES

When the porcelain tile firing cycle is excessively slow during cooling or the hold at peak firing temperature is too long, β phase destabilisation occurs at room temperature. Fig. 8a shows an XRD diagram of a tile glaze that has been cooled more slowly than usual in the industry, with a low concentration of stabilising elements. As a result at room temperature the α -phase appears (Table II). Similarly, Fig. 8b shows an XRD diagram of a tile subjected to heat treatment for 10 h at 1200 °C, in which not only α -cristobalite appears at room temperature but also peaks of tridymite (marked as T1 and T2 in this figure).

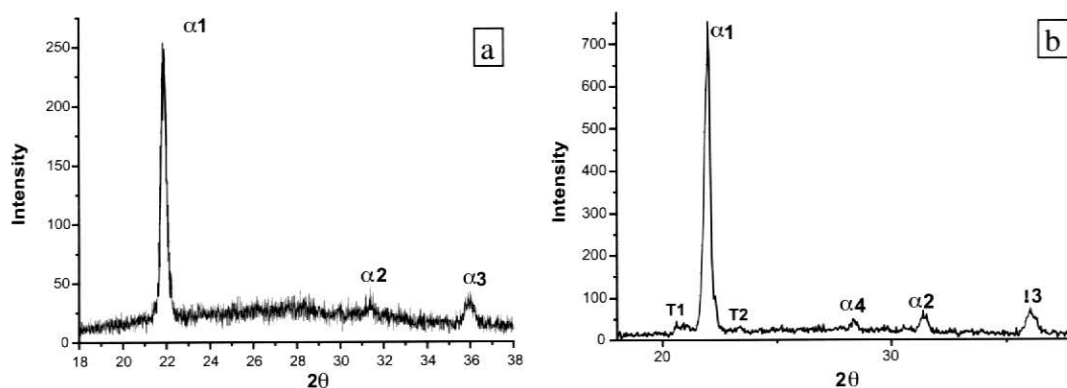


Fig. 8.- XRD diagrams of a glaze that has been cooled slowly (a) the α -cristobalite phase, only three reflections clearly appearing ($\alpha 1$, $\alpha 2$, $\alpha 3$) of the four characteristic reflections in this 2θ range. In (b) a sample is depicted treated at 1200 °C for 10 h, clearly showing the four reflections ($\alpha 1$, $\alpha 2$, $\alpha 3$, $\alpha 4$) together with the two tridymite phase maximums (T1 and T2). The values of the 2θ angles and Å spacings of these reflections are detailed in Table II.

	$\alpha 1$	$\alpha 2$	$\alpha 3$	$\alpha 4$
α -cristobalite SiO ₂ *	21.98, 4.040	31.47, 2.837	36.08, 2.487	28.44, 3.136
α -cristobalite Fig. 8a	21.99, 4.037	31.46, 2.840	36.09, 2.487	-
α -cristobalite Fig. 8b	21.96, 4.044	31.42, 2.845	36.04, 2.480	28.37, 3.143

(*ASTM File no. 39-1425)

Table 2. Values of the 2θ angles and d spacings in Å measured in the mean position of the peak at half height in the XRD diagrams of the samples indicated in the text (Cu K α , radiation)

The appearance of the α -phase in these cases indicates that the $\beta \rightarrow \alpha$ transition has occurred during cooling because the structure of β -cristobalite is metastable, and though it can initially form with great ease, it tends to expel foreign cations from the structure to achieve chemical stability of the SiO₂ phase. Thus, in prolonged heating, the following reaction occurs:

β -cristobalite rich in Al, A⁺, A⁺⁺ \rightarrow SiO₂ β -cristobalite + tridymite rich in Al, A⁺, A⁺⁺
 so that when cooling takes place, the cristobalite with the composition closest to SiO₂ transforms into the α -phase, owing to the absence of stabilising cations.

The formation of poor chemical stabilisation, because of defects in the frit starting chemical composition, effect of prolonged heating or excessively slow cooling, which give rise to the appearance of the α phase at room temperature, has a pronounced macroscopic effect at the glaze surface, giving it a wrinkled and cracked appearance. Fig. 9a shows a glaze that has been held on purpose for long time at peak firing temperature, with crystallisation practically extending over the whole glaze surface. However, cracks are observed across the entire surface. In this case, if regions are sought that still contain a glassy part, it can be observed that they are associated with the crystal-glass contact (marked by an arrow in Fig. 9b). It is clear that this is due to the difference in shrinkage during cooling of the glass and the glaze, which gives rise to crack formation at this contact point, i.e., in the weakest area.

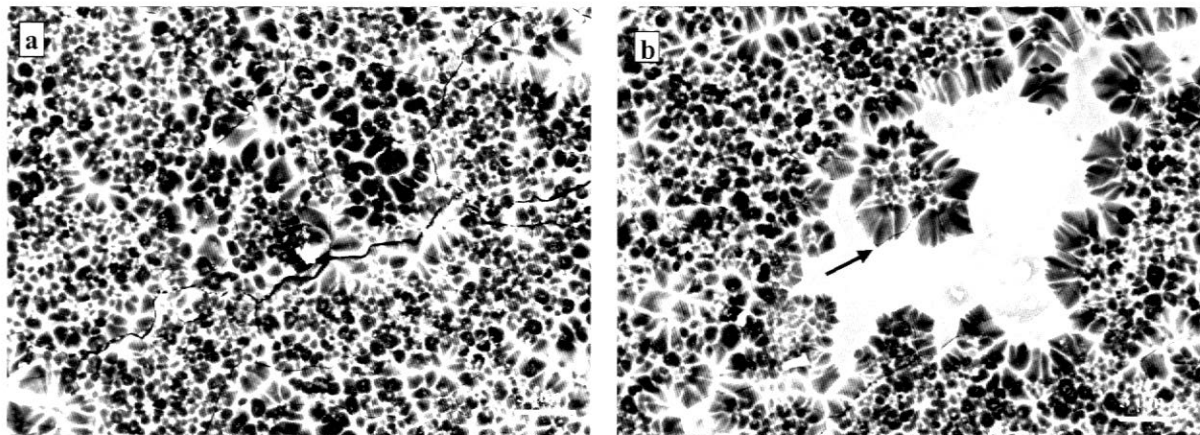


Fig. 9.- SEM micrographs made using the backscattered electron detector with the same magnification (2000x). a) Microtextures observed at the surface of the glaze layer corresponding to the XRD diagram of Fig. 8a, in which fractures are noticed that cross the entire surface of the glaze. b) Microtextures observed at the surface of the glaze layer, with an area of residual glass containing dendritic crystals and microfractures at the crystal-glass interface.

In this figure it can be observed that the crystals have a dendritic morphology, a character that contrasts with the rest of the images where regular isolated crystals or crystal aggregates are mainly found. It can therefore be stated that the initial rate of crystal growth is slower than with crystallisation advance. This is due to the compositional changes of the melt during crystallisation, i.e., as crystallisation advances it becomes richer in B and Na while silica decreases. Thus cationic diffusion is considerably encouraged, increasing the crystal growth rate.

3.6. CERAMIC PROPERTIES OF THE GLASSY AND GLASS-CERAMIC GLAZES

Glass-ceramic glazes, mainly made up of a frit, which is very rich in SiO_2 (which can crystallise chemically stabilised cristobalite CSC), together with industrial minerals (quartz, potassium feldspars, sodium feldspars, kaolin and alumina), can be used for transparent coatings of porcelain tile bodies. The hardness values on the Mohs scale are variable in a range that stretches from over 5 to under 7. The Vickers microhardness values range from 550 to 700 kg/cm^2 , exhibiting higher values than those of conventional transparent glazes and of the polished porcelain tile surface. The chemical resistance tests have shown that the glaze resists acids and bases, and a rating of PEI III is found. Similarly, the glaze polishing processes give rise to high gloss surfaces and great transparency with a notable microtextural quality in the end glaze surface, which provides stain resistance.

4. CONCLUSIONS

In this study conclusions can be drawn concerning two aspects: relative to the characteristics of the materials developed and relative to their industrial application.

4.1. CONCLUSIONS RELATIVE TO THE MATERIALS

i) The crystallisation experiments using the sol-gel method by the coprecipitation technique have enabled verifying that a structure similar to the β cristobalite phase can be stabilised (i.e., CSC) in a wide range of Si substitutions in SiO_2 by Al+Ca or Al+Sr, with heat treatments similar to those involved in porcelain tile firing.

ii) Ceramic frits have been developed in which CSC crystallisation can take place in a wide range of compositions of these frits and under porcelain tile firing cycle conditions. The most interesting compositions are those that are based on the system $\text{SiO}_2\text{-Al}_2\text{O}_3\text{-CaO}$ for CSC crystallisation with additions of other oxides to adapt the behaviour of the frit in terms of required meltability and stretching.

iii) Nucleation is heterogeneous and arises mainly at the glaze surface and at the contacts between frit particles inside the glaze. Crystal growth first produces regular shapes and as the process advances, dendritic crystallisations occur.

iv) The frit can be used to develop glazes comprising this frit and industrial minerals such as quartz, alkaline feldspars, kaolin and alumina.

4.2. RELATIVE TO THE INDUSTRIAL PROCESSES

i) The frits with the capacity to crystallise CSC and form a glass-ceramic glaze can be produced in industrial fritting kilns at temperatures of 1500 °C.

ii) The frits developed can be used together with industrial minerals to prepare glazes (glassy and glass-ceramic) for transparent coatings on porcelain tile bodies in the usual firing cycles employed for manufacturing these materials.

iii) The mechanical and physico-chemical resistance properties of the glazes developed are higher than those of conventional transparent glazes and of these properties in polished porcelain tile surfaces. The glazes enable producing polished surfaces with improved stain resistance compared to polished porcelain tile.

5. REFERENCES

- [1] TICHELL MT, BAKALI J, PASCUAL A, SÁNCHEZ-MUÑOZ L, NEBOT-DÍAZ I, CARDA JB (2000) Esmaltes especiales para soportes de gres porcelánico. *Bol Soc Esp Ceram Vidrio* 39 (1): 31-38
- [2] TICHELL MT, BAKALI J, SÁNCHEZ J, PORTOLÉS J, SOLER C, NEBOT-DÍAZ I, SÁNCHEZ-MUÑOZ L, CARDA JB (2000) Esmaltes vitrocerámicos con cristalizaciones de aluminatos y silicoaluminatos, adaptados a soportes de gres porcelánico. *Qualicer 2000*, P.GI-465-473
- [3] JOVANÍ MA, CARCELLER JV, SOLER A, NEBOT A, NUÑEZ I, SÁNCHEZ-MUÑOZ L, GUAITA J, CORDONCILLO E, CARDA JB (2000) Desarrollo de esmaltes híbridos a partir de fritas y geles, adaptados a ciclos de monococción de gres y gres porcelánico. *Qualicer 2000*, P.GI-199-211
- [4] LEONELLI C, MANFREDINI T, PAGANELLI M, PELLACANI GC, AMORÓS JL, ENRIQUE JE, ORTS MJ, BRUNI S, CARIATI F (1991) $\text{Li}_2\text{O-SiO}_2\text{-Al}_2\text{O}_3\text{-Me}^n\text{O}$ glass ceramic systems for tile glaze applications. *J Am Ceram Soc* 74(5): 983-987
- [5] ESCARDINO A (1997) Vidriados cerámicos de naturaleza vitrocristalina. *Ceram Infor* 231:17-35
- [6] FERRARI AM, BARBIERI L, LEONELLI C, MANFREDINI T, SILIGARDI, CORRADI AB (1997) Feasibility of using cordierite glass-ceramic as tile glazes. *J Am Ceram Soc* 80(7):1757-1766
- [7] BEALL GH, DUKE DA (1986) Transparent glass-ceramics. *J Mater Sci* 4:340-352
- [8] PARTRIDGE G, PHILLIPS SV (1991) A review of transparency in glass ceramics. *Glass Technology* 32(3):82-90
- [9] BALDI G, GENERALI E, LEONELLI C, MANFREDINI T, PELLACANI GC, SILIGARDI C (1995) Effects of nucleating agents on diopside crystallization in new glass-ceramics for tile-glaze application. *Jour Mat Sci* 30(12):3251-3255
- [10] HATCH DM, GHOSE S (1991) The α - β transition in cristobalite, SiO_2 . Symmetry analysis, domain structure, and the dynamical nature of the b-phase. *Phys Chem Mineral* 17:554-562
- [11] SPEARING DR, FARNAN I, STEBBINS JF (1992) Dynamics of the α - β transition in quartz and cristobalite as observed by in-situ high temperature ^{29}Si and ^{17}O NMR. *Phys Chem Mineral* 19:307-321
- [13] SCHMAHL WW, SWAINSON IP, DOVE MT, GRAEMME-BARBER A (1992) Landau free energy and order parameter behaviour of the α/β phase transition in cristobalite. *Zeit Kristall* 201:125-145
- [14] SCHMAHL WW (1993) Athermal transformation behaviour and thermal hysteresis at the SiO_2 - α/β -cristobalite phase transition. *Eur J Mineral* 5:377-380
- [15] PHILIPS BL, THOMPSON JG, XIAO Y, KIRKPATRICK J (1993) Constrains on the structure and dynamics of the β -cristobalite polymorphs of the SiO_2 and AlPO_4 from ^{31}P , ^{27}Al and ^{29}Si NMR spectroscopy to 770K. *Phys Chem Mineral* 20:341-352
- [16] PERROTA AJ, GRUBBS DK, MARTIN ES, DANDO NR, MCKINSTRY HA, HUANG CY (1989) Chemical stabilization of β -cristobalite. *J Am Ceran Soc* 72(3):441-447
- [17] SALTZBERG MA, BORS SL, BERGNA H, WINCHESTER SC (1992) Synthesis of chemically stabilizad cristobalite. *J Am Ceram Soc* 75(1):89-95
- [18] GAI-BOYES P, SALTZBERG MA, VEGA A (1993) Structures and stabilization mechanisms in chemically stabilized ceramics. *Jour Solid State Chem* 106:35-47

- [19] THOMAS ES, THOMPSON JG, WITHERS RL, STERNS M, XIAO Y, KIRKPATRICK RJ (1994) Further investigation of the stabilization of β -cristobalite. J Am Ceram Soc 77(1):49-56
- [20] ALCALÁ MD, REAL C, CRIADO JM (1996) A new "incipient-wetness" method for the synthesis of chemically stabilized β -cristobalite. J Am Ceram Soc 79(6):1681-1684
- [21] MACDOWELL JR (1969) Alpha- and beta-cristobalite glass-ceramic articles and methods. US Pat N° 3.445.252
- [22] LI CT (1978) Glasses termally stable high (beta)-cristobalite glass-ceramics and methods. US Pat N° 4.073.655
- [23] JEAN JH, GUPTA TK (1993) Alumina as a devitrification inhibitor during sintering of borosilicate glass powders. J Am Ceram Soc 76(8):2010-2016
- [24] IMANAKA Y, AOKI S, KAMEHARA N, NIWA K (1995) Cristobalite phase formation in glass/ceramic composites. J Am Ceram Soc 78(5):1265-1271.